Chapter 6 Turbulent Transport and its Modeling

6.1 Molecular Momentum Transport: molecular model viscous effects

$\rho \overline{u_i u_j}$ = turbulent momentum flux

$\rho \overline{uv}$ = x momentum ρv in y direction due to turbulent v; for $\underline{V} = (U+u, v, w)$

Classical ideas for modeling turbulent transport were based on molecular momentum transport for ideal (non-dense) gas: molecules far apart & intermolecular forces weak; molecules far apart in free flight with brief collisions at which time their direction & speed change.

Across plane separating the gas in two regions the molecules do not attract or repel each other (contrary to liquids); therefore, the primary source of shear stress is that due to microscopic transport of momentum due to random molecular motions.

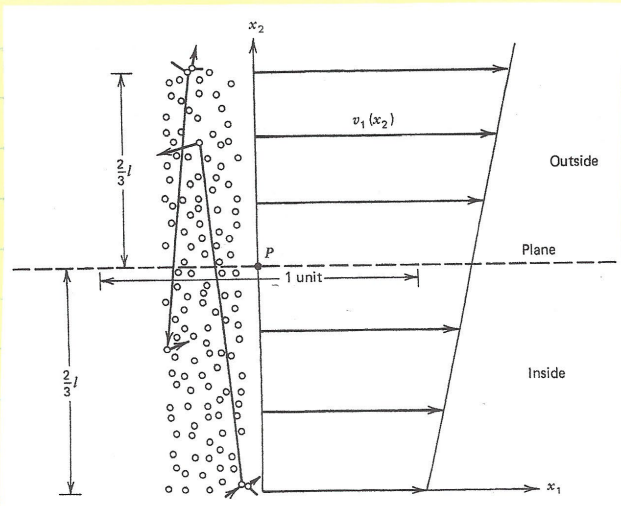

Figure 6.1 Molecular model of the viscosity of a gas.

Newtonian fluid stress rate of strain relationship

$$\tau_{21} = \mu \left(\frac{\partial v_1}{\partial x_2} + \frac{\partial v_2}{\partial x_1} \right)$$

$$= \mu \frac{\partial v_1}{\partial x} \qquad \text{for } \underline{v} = v_1(x_2)\,\hat{e}_1$$

which can be derived for ideal gas using four facts from kinetic theory:

1. Molecules that cross the plane x_2 = constant begin their free flight on average a distance $\pm \frac{2}{3} l$ (l = mean free path) from the plane

2. $l = 1/\sqrt{2}\,\pi d^2 n$ $\qquad$ d = molecular diameter, n = number density

Since molecules have distribution of speeds, accounting relative velocities RHS = 3/4 × RHS; and for Maxwellian distribution of velocities RHS = .707 × RHS

3. Flux of velocities across x_2-plane per unit area $= \frac{1}{4} n \bar{v}$ $\qquad$ $\bar{v}$ = average molecular speed (without regard direction)

4. Average molecular speed

$$\bar{v} = \left[\frac{8kT}{\pi m} \right]^{1/2} = f(T) \qquad k = \text{Boltzmann constant},\ m = \text{molecular mass}$$

Shear stress x_2-plane

$$\tau_{21} = \frac{x_1 \text{ force}}{\text{unit area}} = \text{net flux of momentum across } x_2\text{-plane}$$

Particle flux from above: $m v_1 \Big|_{x_2 + 2/3 l} = m\left[v_1 + \frac{dv_1}{dx_2}\left(\frac{2}{3}l\right) + \cdots\right]_{x_2}$

from below: $m v_1 \Big|_{x_2 - \frac{2}{3} l} = m\left[v_1 + \frac{dv_1}{dx_2}\left(-\frac{2}{3}l\right) + \cdots\right]_{x_2}$

$$\tau_{21} = \frac{1}{4} n \bar{v} \times \left[m v_1(x_2 + 2/3 l) - m v_1(x_2 - 2/3 l) \right]$$

$$= \frac{1}{4} n \bar{v} \times m \frac{4}{3} l \frac{dv_1}{dx_2}$$

ie comparing with $\tau_{ij} = \mu(u_{i,j} + u_{j,i})$

$$\mu = \frac{1}{3} n \bar{v} m l = \frac{2}{3\lambda^2}\left[\frac{mkT}{\pi}\right]^{1/2} = \frac{1}{3} \rho \bar{v} l$$

$= f$ (molecular properties & T)

$\mu \uparrow \quad m \uparrow$

$\mu \downarrow \quad d \uparrow$

$\mu \neq f(p)$

$\mu \uparrow \sqrt{T} \uparrow$ more complete theory includes inter molecular forces & better agreement T dependence

Viscosity liquids needs more advanced modelling considering inter molecular forces, but results in same $\tau_{ij} = \mu(u_{i,j} + u_{j,i})$ relationship

6.2 Model Turbulent Transport by Analogy Molecular Transport

Newtonian fluid (incompressible flow)

$$\sigma_{ij} = -p\delta_{ij} + 2\mu S_{ij} \qquad S_{ij} = \frac{1}{2}(u_{i,j} + u_{j,i})$$
$$= -p\delta_{ij} + \tau_{ij}$$

μ = isotropic viscosity = property of fluid

in analogy the turbulent Reynolds stresses are modeled using the eddy viscosity concept

$$a_{ij} = -\rho\overline{u_i u_j} + \underbrace{\frac{2}{3}\rho k \delta_{ij}}_{\text{isotropic RS}} = \rho\nu_t \underbrace{(U_{i,j} + U_{j,i})}_{\text{mean flow rate of strain}} = \rho\nu_t S_{ij}$$

= anisotropic RS = modeled using isotropic eddy viscosity ν_t or $\mu_t = \rho\nu_t$, which may be contrasted with μ definition for ideal gas; however, no reason to believe turbulent motions are without directional biases that are not aligned with S_{ij}. Nonetheless eddy viscosity concept forms the basis of traditional RANS models, which focuses on the modeling of ν_t.

For example, consider 1D shear flow

$$\tau_{12}/\rho = -\overline{uv} = \nu_t \frac{dU}{dy} \qquad \nu_t = \mu_t/\rho$$

Large scale turbulent eddies are most important in transporting momentum across the flow, which are mostly driven by motion of pressure forces vs. viscosity. Assume $-\rho\overline{uv}$ due to turbulent eddies with transverse size l of intensity characterized by velocity scale u_0.

Assume $A_p \to B$ & vice versa
$B_p \to A$ p = fluid particles
which interact & merge with the flow (transporting momentum)

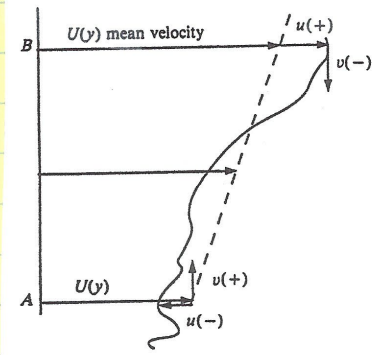

Figure 26.4 Mean velocity profile and the fluctuations that contribute to the Reynolds stresses.

$$-\rho\overline{uv} = f\left(\rho, l, u_0, \frac{dU}{dy}\right)$$

$$-\overline{uv}/u_0^2 = f\left(l/u_0 \frac{dU}{dy}\right)$$

} dimensional analysis

Assume linear relationship of eddy viscosity

$$-\overline{uv} = u_0^2\, c\, l/u_0 \frac{dU}{dy}$$

$$= c\, l\, u_0 \frac{dU}{dy}$$

ie $\quad \nu_t = c\, l\, u_0$

u_0 = turbulent velocity scale
l = turbulent length scale

which is also consistent ideal gas theory

$\mu = \frac{1}{3} \rho \bar{v} l$

the time scale for eddy turnover time is

l / u_0

a time scale for mean flow $\left(\frac{dU}{dy}\right)^{-1}$; therefore assume

$$l / u_0 = \left|\frac{dU}{dy}\right|^{-1}$$

take $$u_0 = l \left|\frac{dU}{dy}\right|$$

$$\nu_t = c\, l^2 \left|\frac{dU}{dy}\right|$$

or $$\mu_t = c \mu \rho\, l^2 \left|\frac{dU}{dy}\right|$$

(1) this approach is the Prandtl mixing length theory. l depends on the type of flow.

$l \propto$ larger scale eddies

Free shear flow: $l = c\delta$ $c = f$(mixing layer, jet, wake)

BL: $l = \kappa y$ i.e. eddy size $\propto y$ near wall

$= c\delta$ away from wall

(2) $k-\varepsilon$ model

$V = \sqrt{k}$ & $l = k^{3/2}/\varepsilon$ = length associated eddy turn over time $t_e = l_e/u_{rms}$

$\mu_t = C_\mu \rho l \, k^{1/2}/\varepsilon$

$\varepsilon = \dfrac{u_{rms}^2}{l_e/u_{rms}} = u_{rms}^3/l_e$

$l_e = \dfrac{u_{rms}^3}{\varepsilon}$

and additional equations model for k & ε. $= k^{3/2}/\varepsilon$

Eddy viscosity concept is based on ideal gas molecular momentum transport; thus, assumes:

1. mixing occurs over well defined mixing time
2. momentum preserved between collisions
3. linear variation V over the mixing length

6.3 Lagrangian Analysis Turbulent Transport

Gradient transport law requires $l \ll$ region over which mean velocity can be assumed linear. For turbulent transport, l determined by eddy size/action $\gg$ molecular mean free path or per molecular viscosity of viscous stress tensor.

Figure shows linear approximation mean velocity profile only valid for very small distances.

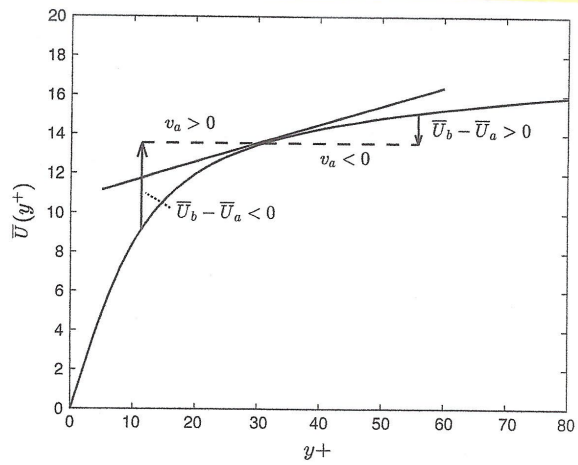

Figure 6.2 A local linear approximation to the mean velocity field $\overline{U}$ at a point a in a channel flow is inappropriate for fluid particles traveling significant distances during the mixing time. Fluid particles traveling toward the wall located at $y^+ = 0$ have $v_a < 0$, $\overline{U}_b - \overline{U}_a > 0$, and vice versa for particles traveling away from the wall.

However, concept that turbulent mixing in which fluid particles carry momentum from initial to final points over a mixing time to cause net momentum transport may have some validity.

To analyze the validity of $\sigma_{12}^T = -\rho\overline{uv} = \mu_t \frac{\partial \overline{U}}{dy}$ using $\underline{v} = \overline{\underline{v}} + \underline{u}$ nomenclature, the turbulent motions that cause u and v to be correlated are explored using DNS data for channel flow.

Figure 6.3 Ensemble of paths, each with a different initial position **b**, arriving at **a**.

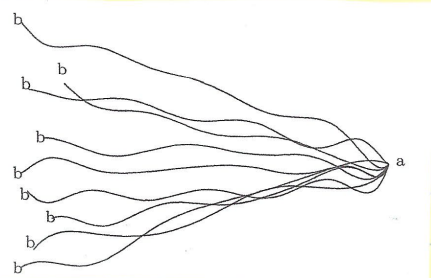

Consider set of particles arriving $\underline{a}$ at time t which originated at $\underline{b}$ following various paths $X(s)$ such that $X(t) = \underline{a}$ & $\underline{X}(t-\tau) = \underline{b}$ where $\underline{X}(s)$ & $\underline{b}$ are random ensemble of realizations. $\tau > 0$ = motion at earlier times than t.

$$\frac{d\underline{X}}{ds}(s) = \underline{U}(\underline{X}(s), s) = \overline{U}(\underline{X}(s), s) + \underline{u}(\underline{X}(s), s)$$

Lagrangian Eulerian Ensemble average where both terms are random since $\underline{X}(s)$ is random

$$\underline{U}_a = \overline{\underline{U}}_a + \underline{u}_a \quad @\ t$$

$$\underline{U}_b = \overline{\underline{U}}_b + \underline{u}_b \quad @\ t-\tau$$

$$\int_{t-\tau}^{t} d\underline{X}(s) = \int_{t-\tau}^{t} \underline{U}(\underline{X}(s), s)\, ds$$

$\underline{a} - \underline{b} = \underline{L}$ = change in particle position from $\underline{b}$ to $\underline{a}$ in time τ

Using $\underline{U}_a$ & $\underline{U}_b$ equations:

$$u_a = u_b + \underbrace{(\overline{U}_b - \overline{U}_a)}_{①} + \underbrace{(U_a - U_b)}_{②}$$

① = change in mean velocity field

② = change in velocity due acceleration or deceleration caused by pressure & viscous forces

Express u_a in terms of values at earlier time + factors that led to its change.

Thus even for $v_a = \bar{v}_b$ i.e. non accelerating particles $u_a \neq u_b$ due to changes in local mean velocity.

$$\overline{u_a v_a} = \underset{①}{\overline{u_b v_a}} + \underset{②}{\overline{v_a(\bar{v}_b - \bar{v}_a)}} + \underset{③}{\overline{v_a(v_a - \bar{v}_b)}}$$

For small τ $\overline{u_a v_a} = \overline{u_b v_a}$, whereas for large τ $\overline{u_b v_a} = 0$, which gives upper limit for mixing time.

$\overline{\underline{\tau}}_D$ = displacement transport term = ② represents momentum transport due to eddy mixing over time interval for which $\overline{u_a v_a}$ is created. If locally mean velocity is linear this term will yield gradient diffusion/viscosity model

< 0

Since for $v_a < 0$
$\bar{v}_b - \bar{v}_a > 0$ &
for $v_a > 0$ $\bar{v}_b - v_a < 0$

③ is absent in molecular model (& gradient model) since molecules are assumed to retain their momentum over the mixing time.

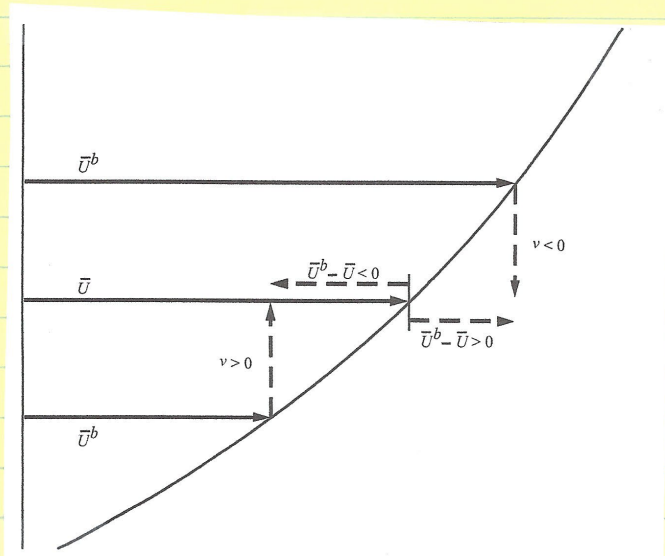

Fig. 6.7 Source of displacement transport correlation.

Channel Flow
DNS

$y^+ = y v_\tau / \nu$

$v_\tau = \left[\nu \frac{d\bar{U}}{dy}(0) \right]^{1/2}$

= friction velocity

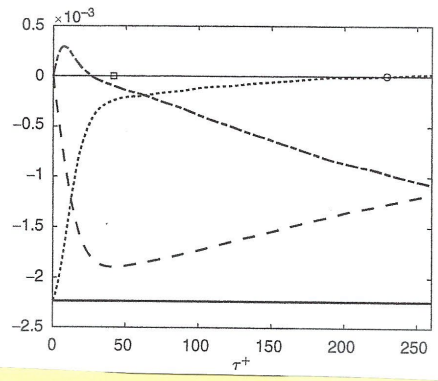

Figure 6.4 Decomposition in Eq. (6.24) at $y^+ = 54.8$. $\cdots$, $\overline{u_b v_a}$ with zero point, τ_m, denoted by a circle; $--$, $\overline{v_a(\bar{U}_b - \bar{U}_a)}$ with minimum denoted by a square; $-\cdot-$, $\overline{v_a(U_a - U_b)}$; $—$, $\overline{u_a v_a}$.

$\overline{u_b v_a} = 0$ for large $\tau^+ = t v_\tau / y^+$. $\bar{q}_D$ minimum where $\overline{u_b v_a}$ is some magnitude. $\overline{u_a v_a}$ is at τ_D = mixing time or reflects most closely idea of gradient hypothesis.

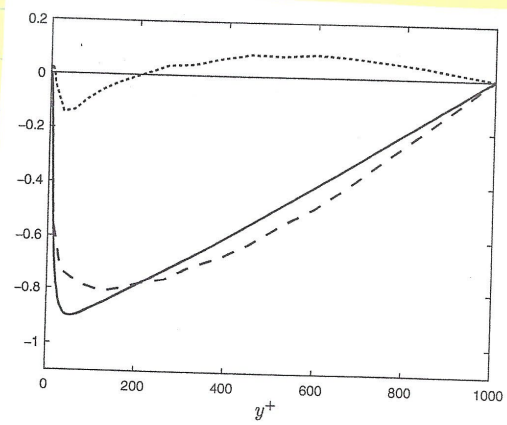

lower half of channel

Figure 6.5 Evaluation of Eq. (6.24) at τ_D computed across the channel. $—$, $\overline{u_a v_a}$; $--$, $\overline{(\bar{U}_b - \bar{U}_a) v_a}$; $\cdots$, $\overline{(U_a - U_b) v_a} + \overline{u_b v_a}$.

$\overline{u_a v_a} <$ = transport u towards wall

Shows $\overline{u_a v_a} \approx \bar{q}_D$ & ① + ③ only small effect

6.4 Transport Producing Motions

N points that lead to $\overline{u_a v_a} < 0$ ie u_a & v_a opposite sign must be greater than those events same sign

(a) rank from most + to most −

(b) partial sums $\sum u_a^i v_a^i$ point in reached N_0 where sign changes from + to − ∴ $N > N_0$ responsible $\overline{uv} < 0$ since other contributions cancel out between + & −. Fraction $(N-N_0)/N$ reveals useful information how $\overline{uv}$ created.

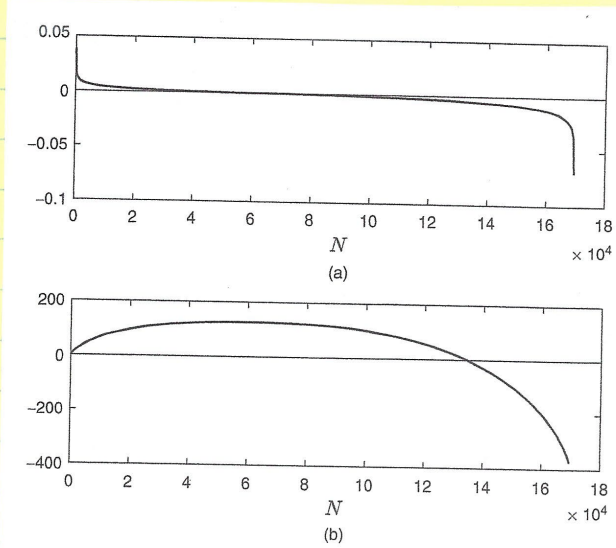

Figure 6.6 Contributions to $\overline{uv}$ at $y^+ = 84.8$ from a data set consisting of 169,344 points in the lower channel half. (a) Individual contributions ranked from largest to smallest. (b) Cumulative sum of contributions in (a) showing zero crossing at $N_0 = 134{,}543$.

$\overline{u_a v_a}$ terms ①, ② & ③ for $(N-N_0)/N$ fraction of events. For large portion channel $\overline{u_a v_a}$ & ② follow same trend. Fraction is generally 20% & rises to 30% at $y^+ = 30$ & all terms drop 0 at center due + − cancellation due symmetry

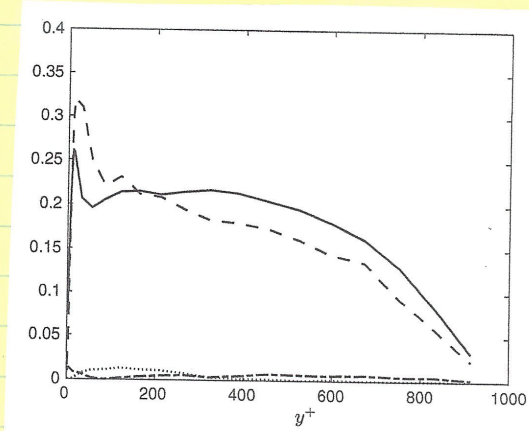

Figure 6.7 Fraction of points in the data ensembles that account for the local computed values of the terms in Eq. (6.24). —, $\overline{u_a v_a}$; – –, $\overline{(\overline{U}_b - \overline{U}_a)v_a}$; – · –, $\overline{(U_a - U_b)v_a}$; · · · , $\overline{u_b v_a}$.

shows $\overline{u_b v_a}$ & $\overline{v_a(U_a - U_b)}$ & relatively rare events <1%

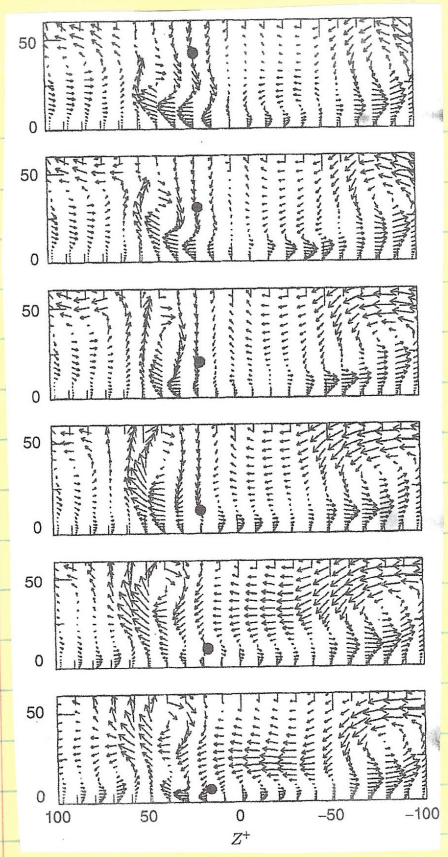

Figure 6.8 Fluid particle arriving at $y^+ = 7.3$ [7] due to a sweep event. Time increases moving from top to bottom image. Reprinted with the permission of Cambridge University Press.

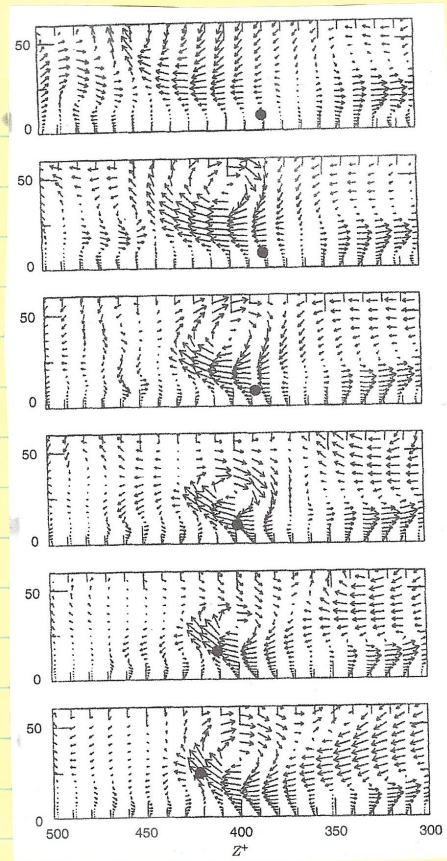

Figure 6.9 Fluid particle arriving at $y^+ = 24.6$ [7] due to an ejection event. Time increases moving from top to bottom image. Reprinted with the permission of Cambridge University Press.

Events that make signif pos contribution are vortical eddies with streamwise orientation

Sweep event : high speed flow toward wall, dominant contribution in buffer layer

Ejection event : low speed flow ejected outward occurs outside buffer layer

Mixing time = time duration coherent vortices exert influence

6.5 Gradient Transport

If gradient transport is valid, it should be due $\underline{\tau}_D$ under further hypothesis that change in mean velocity along particle path is linear.

$$\underline{s} = \underline{a} - \underline{L}$$

$$\overline{U}_s = \overline{U}(\underline{a} - \underline{L}) = \overline{U}_a - L_2 \frac{d\overline{U}}{dy} + \cdots$$

$$\overline{\tau}_D = \overline{v(\overline{U}_s - \overline{U}_a)} = \overline{-v L_2} \frac{\partial \overline{U}}{dy} + \cdots \qquad \underline{L} = \int_{t-\tau}^{t} \underline{U}(\underline{X}(s), s)\, ds$$

Thus $\nu_t = \overline{-v L_2}$

Define Lagrangian auto-correlation fuction

$$f_{vv}(s) = \frac{\overline{v(\underline{X}(t), t)\, v(\underline{X}(t+s), t+s)}}{\overline{v(\underline{X}(t), t)^2}}$$

$$\nu_t = \overline{v^2}\, T_{22} \qquad T_{22} = \int_{-\infty}^{0} f_{vv}(s)\, ds = \text{Lagrangian integral scale}$$

where $f_{vv}(s) = 0$ for $|s|$ large

If $\nu_t = \dfrac{-\overline{uv}}{d\overline{U}/dy}$ then $\nu_t = \overline{v^2} T_{22}$ should be valid

Some discrepancies for $y^+ > 500$ where physical ν_t = constant & modeled decreases; at near wall where physical < modeled

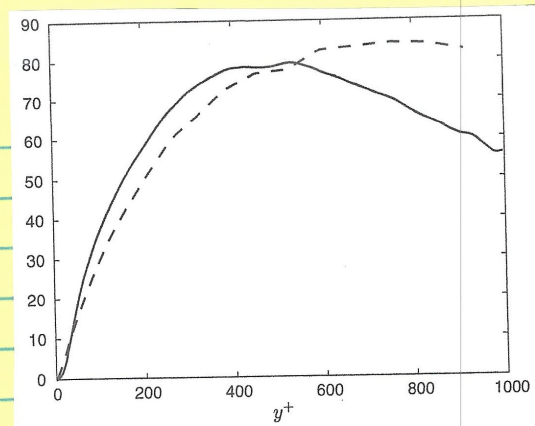

Figure 6.10 Eddy viscosity in channel flow: ––, $\mathcal{T}_{22}^{+}\overline{v^2}^{+}$; —, ν_t^+.

Obvious differences gradient transport vs actual $\overline{uv}$

Large differences near wall, whereas smaller in outer part ∴ more suitable central part

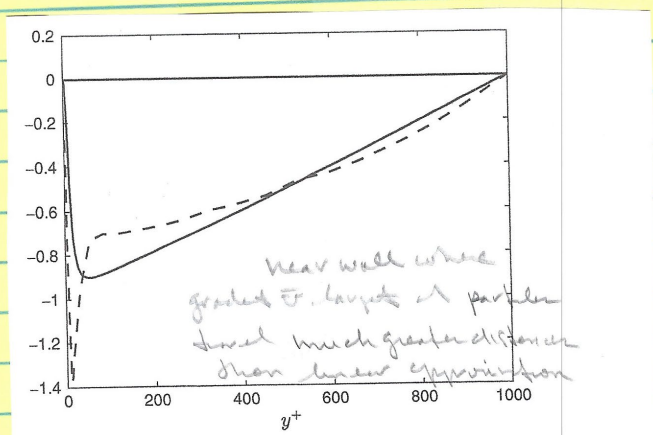

Figure 6.11 Inadequacy of gradient transport physics: —, $\overline{uv}^+$; ––, $-\mathcal{T}_{22}^{+}\overline{v^2}^{+}\, d\overline{U}^+/dy^+$.

note $\nu_t > 0$ over whole domain as per $d\bar{U}/dy$ except center channel where both = 0

However not satisfied for rough wall & ν_t shows unphysical behavior; & numerical methods unstable for $\nu_t < 0$

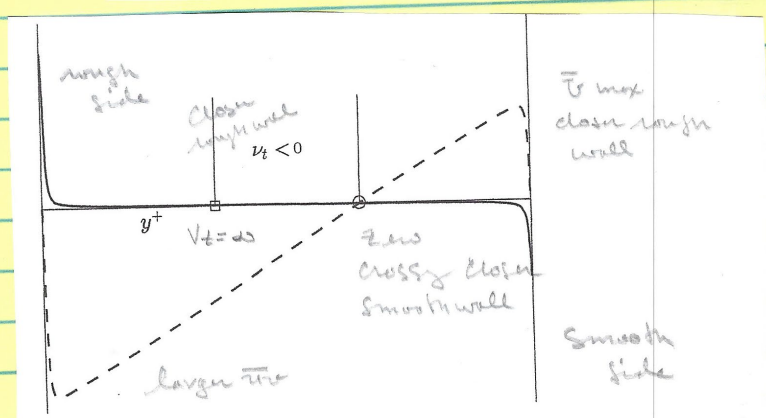

Figure 6.12 A region of negative eddy viscosity can be expected in a channel flow with one rough wall (on the left) and one smooth wall (on the right). —, $d\overline{U}/dy$; ––, $\overline{uv}$; □, zero crossing of $d\overline{U}/dy$; ○, zero crossing of $\overline{uv}$.

6.6 Homogeneous Shear Flow

Ideal flow: $S = \frac{d\bar{U}}{dy} > 0$ = Constant + homogeneous / isotropic turbulence

Should offer opportunity assess gradient transport model, since no higher elevations $\bar{U}$. Also

$$\overline{v_a(U_A - U_B)} = -\int_{t-T}^{t} \overline{v \frac{\partial \bar{P}}{\partial x}(s)}\,ds + \int_{t-T}^{t} \overline{\nu \nabla^2 U(s)}\,ds$$ likely small

K equation takes form

$$\frac{dK}{dt} = P - \varepsilon \qquad P = -\overline{uv}\frac{d\bar{U}}{dy} > 0 \text{ since } \overline{uv} < 0 \text{ \& } S > 0$$

ε equation takes form

$$\frac{d\varepsilon}{dt} = P_\varepsilon^1 + P_\varepsilon^2 + \underbrace{P_\varepsilon^4 - Y_\varepsilon}_{\text{Same as isotropic decay due homogeneous/isotropic turbulence assumption}}$$

For homogeneous shear flow:

$$P_\varepsilon^1 + P_\varepsilon^2 = -2\nu\overline{\omega_1\omega_2}\,S \qquad \text{since } \overline{u_{i,m}u_{j,n}} = \overline{u_{i,n}u_{j,m}}$$

$$\frac{\overline{\omega_1\omega_2}}{S} \simeq \frac{\overline{uv}}{2K}$$

$$P_\varepsilon^1 + P_\varepsilon^2 = C_{\varepsilon 1} P \frac{\varepsilon}{K} \qquad \varepsilon = \nu S$$

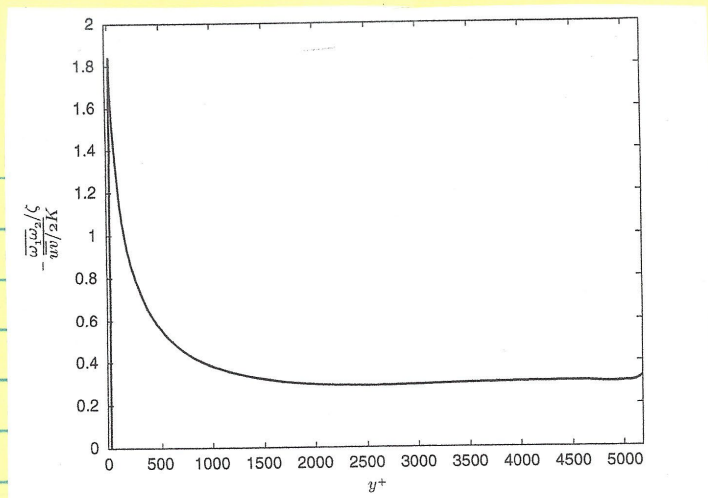

Figure 6.13 Demonstration of the near constancy of $(\overline{\omega_1\omega_2}/\zeta)/(\overline{uv}/2K)$ in the central region of channel flow for $R_\tau = 5186$. Data taken from [10].

$$P_\zeta^* - Y_\zeta = S_K^* R_T^{1/2} \frac{\zeta^2}{K} - G^* \frac{\zeta^2}{K}$$

$$G^* = (S_K^* - C_{\zeta 3}) \sqrt{R_T} + C_{\zeta 2}$$ assuming rapidly stretching but prevented by dissipation

($C_{\zeta 3} = 0$ in usual RANS models)

$$\frac{d\zeta}{dt} = C_{\zeta 1} P \frac{\zeta}{K} + C_{\zeta 2} R_T^{1/2} \frac{\zeta^2}{K} - C_{\zeta 3} \frac{\zeta^2}{K} \qquad R_T = K^2/\nu\zeta$$

$$+ \frac{dK}{dt} = P - \zeta$$ usual model eqn $\qquad P = -\overline{uv}\frac{dU}{dy}$

EFD & DNS show exponential growth $K \propto \zeta$, but $St < 30$.

Thus, $SK/\zeta = 6$

asymptotic values $\quad P/\zeta = 1.8$

Although LES still not converged $St = 30$

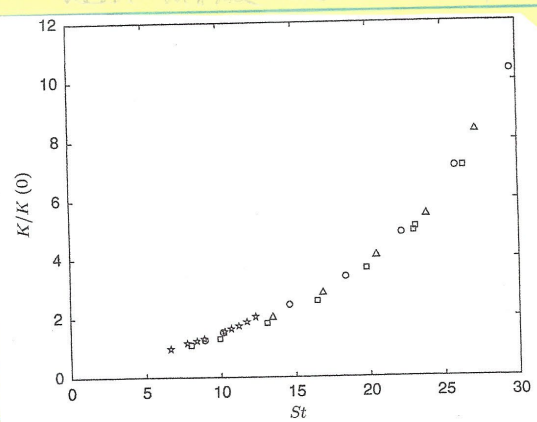

Figure 6.14 Measured $K/K(0)$ in homogeneous shear flow for $St < 30$ from [15]. Reprinted with permission of Cambridge University Press.

Using $t^* = St$ & $K^*(t^*) = K(t)/K(0)$

$$\frac{dK^*}{dt^*} = \frac{\varepsilon}{SK}\left(P/\varepsilon - 1\right)K^*$$ & asymptotic values for ε/SK & P/ε

$$K^*(t^*) = e^{.13 t^*}$$

with similar analysis ε equation (& $c_{\varepsilon 3} = 0$) resulting in exponential growth $\varepsilon^*(t^*)$ Problem 6.2

Long time EFD or similarity not achievable. Two hypotheses put forward:

(1) $P = \varepsilon$ such that K & ε asymptote to constant values Townsend (1956)

(2) K & ε continue exponential growth, which is not physical or unlimited growth K unrealistic

To solve K & ε equations for long time growth the model needed.

$\overline{uv} = -T_{22}\overline{v^2}S$ where for isotropic flow $\overline{v^2} = 2K/3$

assume T_{22} $\propto$ eddy turnover time K/ε
Same as K-ε model: $T_{22} = \frac{3}{2} c_\mu K/\varepsilon$

$$\frac{dK}{dt} = C_\mu \frac{K^2}{\varepsilon} S^2 - \varepsilon$$

$$\frac{d\varepsilon}{dt} = C_{\varepsilon_1} C_\mu K S^2 + C_{\varepsilon_3} R_T^{1/2} \frac{\varepsilon^2}{K} - C_{\varepsilon_2} \frac{\varepsilon^2}{K}$$

$C_{\varepsilon_1} = 1.45$ Same value as isotropic turbulence

self similarity solutions

$C_\mu = .09$ & $C_{\varepsilon_2} = 1.9$ Same values used

near-wall BL

$C_{\varepsilon_3} = 0 \Rightarrow$ no vortex stretching

$= .1 \Rightarrow$ overstretch effects vortex stretch

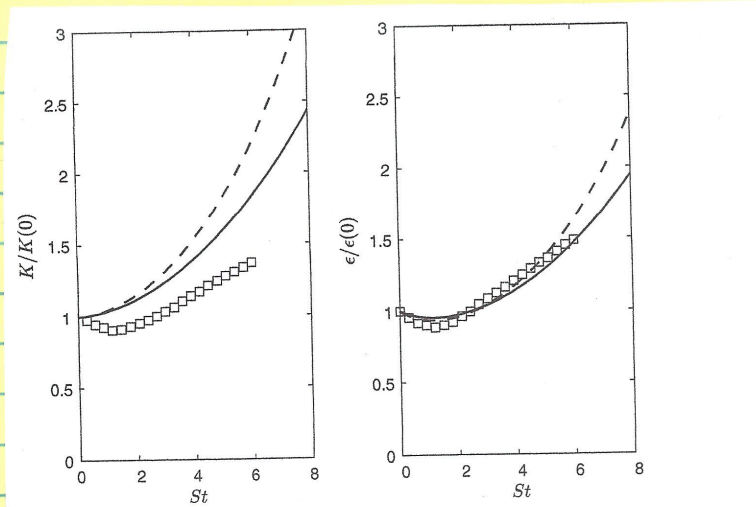

Figure 6.15 Computed solution for $K/K(0)$ (left) and $\epsilon/\epsilon(0)$ (right) in homogeneous shear flow: —, with vortex stretching; – –, without vortex stretching; o, LES calculation [17].

Short time solutions similar EFD

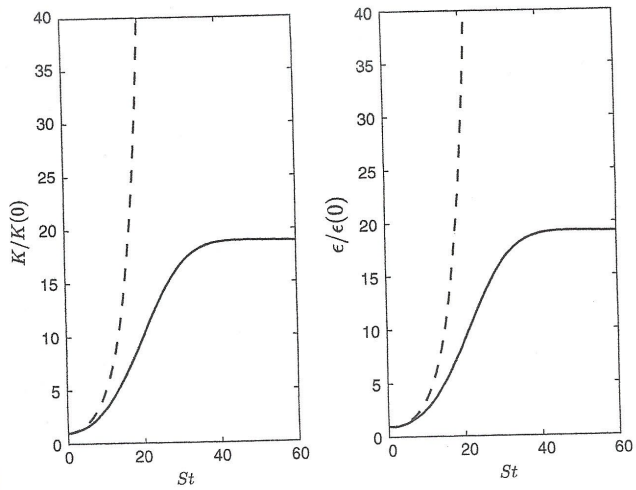

Figure 6.16 Computed solutions for $K/K(0)$ (left) and $\epsilon/\epsilon(0)$ (right) in homogeneous shear flow: —, with vortex stretching; – –, without vortex stretching.

Long time solutions show continued exponential growth for $c_{\xi_3} = 0$, whereas for $c_{\xi_3} \neq 0$ growth curtails at $P = \varepsilon$ equilibrium achieved as per Townsend

Asymptotic values found from setting dk/dt & $d\varepsilon/dt = 0$: $K_\infty = \dfrac{\sqrt{c_\mu}\,(c_{\xi_2} - c_{\xi_1})^2}{c_{\xi_3}^2}\,\nu S$

$$\varepsilon_\infty = \frac{c_\mu\,(c_{\xi_2} - c_{\xi_1})^2}{c_{\xi_3}^2}\,\nu S^2$$

Magnitudes increase with c_{ξ_3}, which highlights importance vortex stretching as an additional source of dissipation

$c_{\xi_3} \neq 0$ that most realistic physics i.e. vortex stretching maintains independent physical processes.

Homogeneous Shear Flow (Pope 5.4.5)

Homogeneous: $\underline{U}(\underline{x},t)$ statistically invariant under translations ie shifts in the origin of the coordinate system

$\underline{u}(\underline{x},t)$ & $p'(\underline{x},t)$ statistically homogeneous; & $\bar{U}_{i,j}$ = uniform but may be $f(t)$

Isotropic: Also invariant under rotations & reflections

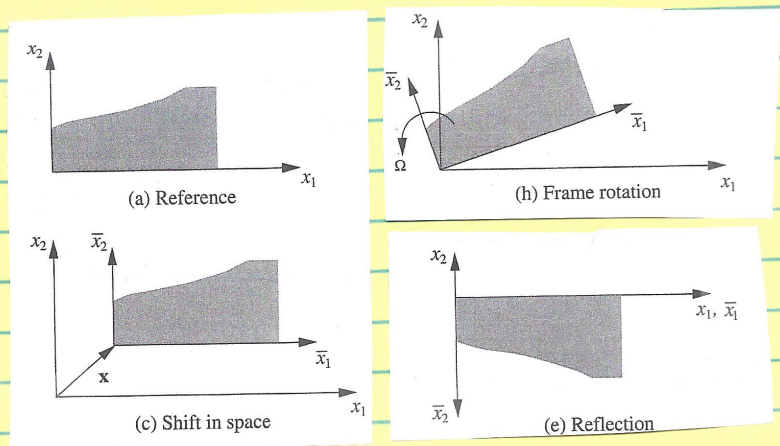

For homogeneous turbulence: $\frac{dk}{dt} = P - \varepsilon$

such that $\tau/2 \frac{dk}{dt} = P/\varepsilon - 1$ $\quad \tau = k/\varepsilon$

which has solution $k(t) = k(0) \exp\left[t/\tau\,(P/\varepsilon - 1)\right]$

Since $P/\varepsilon \approx 1.7 > 1$, $k(t)$ grows exponentially

& also ε & $L = k^{3/2}/\varepsilon = k^{1/2}/\tau$ grow exponentially

Wind Tunnel Experiments

$\bar{U} = S(y)$ $\bar{V} = \bar{W} = 0$

$S = \bar{U}_y$ = constant

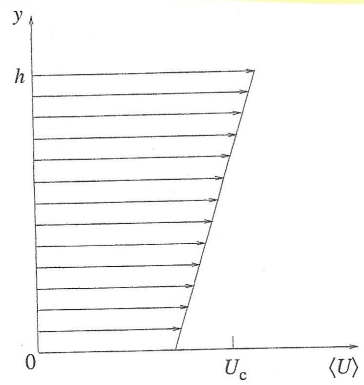

Fig. 5.30. A sketch of the mean velocity profile in homogeneous shear flow.

In spite of axial variation, in frame of reference moving at U_c, $\overline{u_i u_j}$ ~ homogeneous

After initial development time flow becomes self-similar when statistics normalized by S & $k(t)$ become independent of t

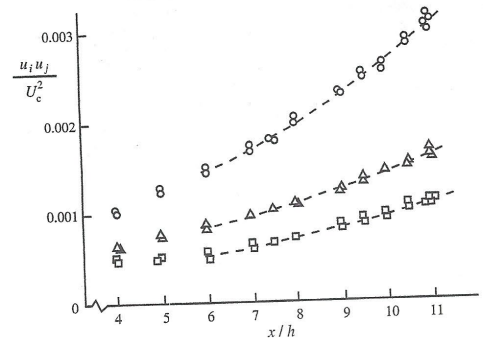

Fig. 5.31. Reynolds stresses against axial distance in the homogeneous-shear-flow experiment of Tavoularis and Corrsin (1981): ○, $\langle u^2 \rangle$; □, $\langle v^2 \rangle$; △, $\langle w^2 \rangle$.

Between $x/h = 7$ & 11 $k(t)$ increases by 65% yet normalized values nearly constant

Table 5.4. *Statistics in homogeneous turbulent shear flow from the experiments of Tavoularis and Corrsin (1981) and the DNS of Rogers and Moin (1987)*

	Tavoularis and Corrsin		Rogers and Moin
	$x/h = 7.5$	$x/h = 11.0$	$St = 8.0$
$\langle u^2 \rangle / k$	1.04	1.07	1.06
$\langle v^2 \rangle / k$	0.37	0.37	0.32
$\langle w^2 \rangle / k$	0.58	0.56	0.62
$-\langle uv \rangle / k$	0.28	0.28	0.33
$-\rho_{uv}$	0.45	0.45	0.57
Sk/ε	6.5	6.1	4.3
$\mathcal{P}/\varepsilon$	1.8	1.7	1.4
$L_{11}S/k^{1/2}$	4.0	4.0	3.7
$L_{11}/(k^{3/2}/\varepsilon)$	0.62	0.66	0.86

τ = turbulent time scale nearly constant such that $S\tau$ ~ constant. L_{11} increases by 300%, but when normalized nearly constant

6.7 Vorticity Transport

$$\frac{\partial \bar{\omega}_i}{\partial t} + \bar{U}_j \frac{\partial \bar{\omega}_i}{\partial x_j} = -\frac{\partial (\bar{P}/\rho + K)}{\partial x_i} + \nu \nabla^2 \bar{\omega}_i + \varepsilon_{ijk} \overline{u_j \omega_k}$$

since $\frac{\partial \overline{u_i u_j}}{\partial x_j} = \frac{\partial K}{\partial x_i} - \varepsilon_{ijk} \overline{u_j \omega_k}$ $\qquad \omega_i = \Omega_i - \bar{\Omega}_i$

where ε_{ijk} is the alternating tensor $= 0$ any two equal
$+1$ ijk cyclic
-1 ijk anticyclic

cyclic 123, 231, 312
anti 321, 213, 132

note that δ_{ij} & ε_{ijk} are the only isotropic 2nd and 3rd order tensors & there are no isotropic 1st order tensors

$\varepsilon_{ijk} = \varepsilon_{jki}$ and $\varepsilon_{ijk} = \varepsilon_{kij}$ is unchanged by moving indices two places right or left, whereas movement one place changes sign $\varepsilon_{ijk} = -\varepsilon_{ikj}$

Also note epsilon delta relationship:

$$\sum_{k=1}^{3} \varepsilon_{ijk} \varepsilon_{klm} = \varepsilon_{ijk} \varepsilon_{klm} = \delta_{il}\delta_{jm} - \delta_{im}\delta_{jl}$$

Returning to rotational form RANS equation in which $(\overline{u_i u_j})_j$ replaced by the vorticity flux $\overline{u_i \omega_j}$ = rate at which ω_j transported in ith direction by u_i

$\bar{P}/\rho + K$ can be solved similarly as $\bar{P}$ alone since $K = 0$ on boundaries forces & moments readily obtained

Assume uni directional channel flow where $\underline{\bar{U}} = (\bar{U}, 0, 0)$ and $\underline{\bar{\Omega}} = (0, 0, \bar{\Omega}_3)$ such that

$$0 = -\frac{1}{\rho}\frac{\partial \bar{p}}{\partial x} + \nu \frac{d^2 \bar{U}}{dy^2} + \overline{v\omega_3} - \overline{w\omega_2}$$

Gradient transport law: $\overline{v\omega_3} = -\overline{vL_2}\,\frac{d\bar{\Omega}_3}{dy}$ with $\overline{vL_2} = \overline{v^2}\,T_{22}$ Same as momentum gradient transport since ν_t independent quantity being transported.

$$0 = -\frac{1}{\rho}\frac{\partial \bar{p}}{\partial x} + \left(\nu + \overline{v^2}\,T_{22}\right)\frac{d^2 \bar{U}}{dy^2} \qquad \bar{\Omega}_3 = -\frac{d\bar{U}}{dy}$$

note $\overline{w\omega_2} = 0$ for purely 2D flow and for gradient transport when $\bar{\Omega}_2 = 0$. Compare with similar equation using $(\overline{u_i u_j})_t$ gradient transport model

$$0 = -\frac{1}{\rho}\frac{\partial \bar{p}}{\partial x} + \frac{d}{dy}\left(\left(\nu + \overline{v^2}\,T_{22}\right)\frac{d\bar{U}}{dy}\right)$$

Shows that vorticity transport ν_t is not differentiated; however, there are difficulties near boundaries since the vorticity flux and $\frac{d\bar{\Omega}}{dy}$ are counter gradient (not compatible) as shown DNS.

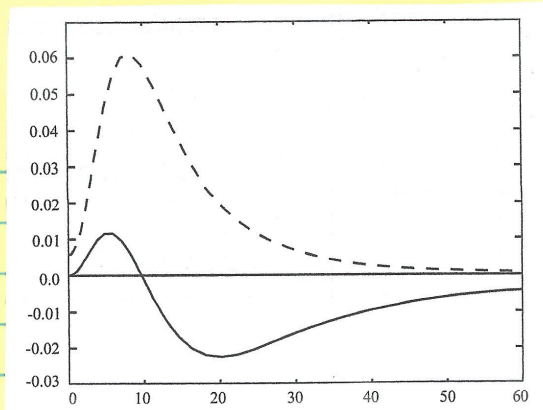

Fig. 6.17 Wall-normal vorticity flux in channel flow. —, $\overline{v\omega_3}$; – –, $d\overline{\Omega}/dy$.

As per bursts $\omega_i^a = \Omega_i^a - \overline{\Omega}_i^a$ $\quad \omega_i^b = \Omega_i^b - \overline{\Omega}_i^b$

momentum transport:

$$\omega_i^a - \omega_i^b = \left(\overline{\Omega}_i^b - \overline{\Omega}_i^a\right) + \left(\Omega_i^a - \Omega_i^b\right)$$

$$\frac{D\Omega_i}{Dt} = \frac{\partial \Omega_i}{\partial t} + v_j \frac{\partial \Omega_i}{\partial x_j} = \Omega_j \frac{\partial v_i}{\partial x_j} + \nu \nabla^2 \Omega_i$$

$$\Omega_i^a - \Omega_i^b = \underbrace{\int_{t-\tau}^{t} \Omega_k(s) \frac{\partial v_i}{\partial x_k}(s)\, ds}_{\text{vortex stretching } (1)} + \underbrace{\int_{t-\tau}^{t} \nabla^2 \Omega_i \, ds}_{\text{viscous effects } (2)}$$

Using these results to evaluate the vorticity flux

$$\overline{v_i^a \omega_j^a} = \overline{v_i\left(\overline{\Omega}_j^b - \overline{\Omega}_j^a\right)} + (1) + (2)$$

assuming τ sufficiently large $\overline{v_i^a \omega_j^b} = 0$

$$\overline{v_i\left(\overline{\Omega}_j^b - \overline{\Omega}_j^a\right)} = -\int_{t-\tau}^{t} \overline{v_i v_k(s)}\, ds \, \frac{\partial \overline{\Omega}_j}{\partial x_k} + \cdots$$

displacement transport term; using Taylor series for $\overline{\Omega}_j^b$

$$(1) = \int_{t-\tau}^{t} \overline{v_i \frac{\partial v_i}{\partial x_k}(s)}\, ds \, \overline{\Omega}_k + \cdots$$

Substituting mean and fluctuating quantities for $v_i(s)$ and $\frac{\partial v_i}{\partial x_j}(s)$

Omitted terms include those that contain only fluctuations, nonlinear in mean flow, $\frac{\partial \bar{U}_i}{\partial y_i}$ which equals zero in simple shear flow, and dissipation term

$$\overline{u_i^a \omega_j^a} = \underbrace{-\int_{t-\tau}^{t} \overline{u_i u_l(s)}\, ds \, \frac{\partial \bar{U}_j}{\partial x_l}}_{\text{gradient term}} + \underbrace{\int_{t-\tau}^{t} \overline{u_l \frac{\partial u_i}{\partial x_l}(s)}\, ds \, \bar{\Omega}_l}_{\text{vortex stretching term}}$$

Lagrangian correlation coefficients:

$$\overline{u_\alpha u_\beta}\, T_{\alpha\beta}(\tau) = \int_{t-\tau}^{t} \overline{u_\alpha(\underline{x}, t)\, u_\beta(\underline{X}(s), s)}\, ds$$

$$\overline{u_\alpha \frac{\partial u_\beta}{\partial x_\gamma}}\, Q_{\alpha\beta\gamma}(\tau) = \int_{t-\tau}^{t} \overline{u_\alpha \frac{\partial u_\beta}{\partial x_\gamma}(s)}\, ds$$

$$\overline{u_\alpha \omega_\beta} = -T_{\alpha k}\, \overline{u_\alpha u_k}\, \frac{\partial \bar{\Omega}_\beta}{\partial x_l} + Q_{\alpha\beta l}\, \overline{u_\alpha \frac{\partial u_\beta}{\partial x_k}}\, \bar{\Omega}_k$$

6.7.1 Vorticity Transport in Channel Flow

$\bar{U}(y) \wedge \bar{\Omega}_3 = -d\bar{U}/dy$

$$\overline{u\omega_1} = \overline{v\omega_2} = \overline{w\omega_3} = \overline{u\omega_2} = \overline{v\omega_1} = 0$$

$$\overline{w\omega_1} = Q_{313}\,\overline{w\frac{\partial u}{\partial z}}\,\overline{\Omega_3}$$

$$\overline{w\omega_2} = Q_{323}\,\overline{w\frac{\partial v}{\partial z}}\,\overline{\Omega_3}$$

$$\overline{v\omega_3} = -T_{22}\,\overline{v^2}\,\frac{d\overline{\Omega_3}}{dy} + Q_{233}\,\overline{v\frac{\partial w}{\partial z}}\,\overline{\Omega_3}$$

$$\overline{u\omega_3} = -T_{12}\,\overline{uv}\,\frac{d\overline{\Omega_3}}{dy} + Q_{133}\,\overline{u\frac{\partial w}{\partial z}}\,\overline{\Omega_3}$$

$$\overline{uv}\,T_{12}(\tau) = \int_{t-\tau}^{t} \overline{u(\underline{x},t)\,v(\underline{X}(s),s)}\,ds$$

$$w\frac{\partial u}{\partial z}\,Q_{313}(\tau) = \int_{t-\tau}^{\tau} \overline{w(\underline{x},t)\,\frac{\partial u}{\partial z}(\underline{X}(s),s)}\,ds$$

with similar definitions for Q_{323}, Q_{233} & Q_{133}

Using DNS best fit data as shown in figures use $T_{22}^+ = 4.8$, $T_{12}^+ = 12.3$, $Q_{233}^+ = 5.5$, $Q_{313}^+ = 9.5$ & $Q_{133}^+ = 16.3$; thus indicating vortex stretching terms are essentially of the turbulent vorticity flux can be accounted for. Gradient terms subtracting away from wall & stretching terms account for non gradient transport for $\overline{v\omega_3}$ & $\overline{u\omega_3}$. $\overline{w\omega_1}$ & $\overline{w\omega_2}$ show effects vortex stretching.

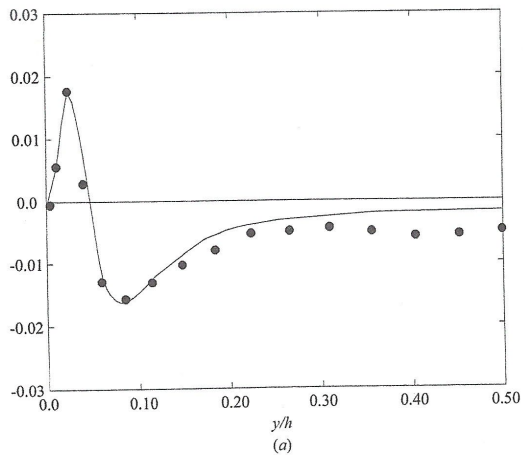

Fig. 6.18 *Predicted vorticity fluxes: •, DNS results; —, prediction from Eqs. (6.39) through (6.42). (a)* $\overline{v\omega_3}$. *(From [1]. Copyright © Springer-Verlag.)*

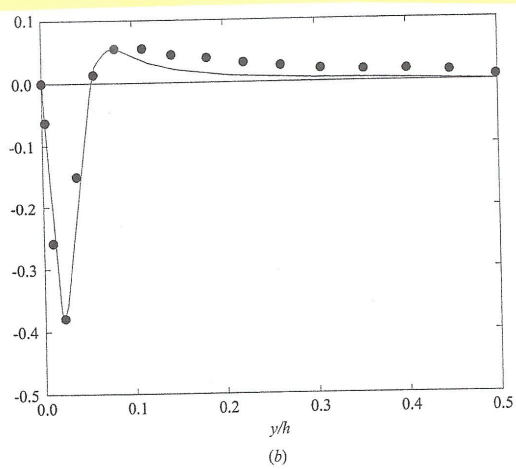

Fig. 6.18 *Predicted vorticity fluxes: •, DNS results; —, prediction from Eqs. (6.39) through (6.42). (b)* $\overline{u\omega_3}$. *(From [1]. Copyright © Springer-Verlag.)*

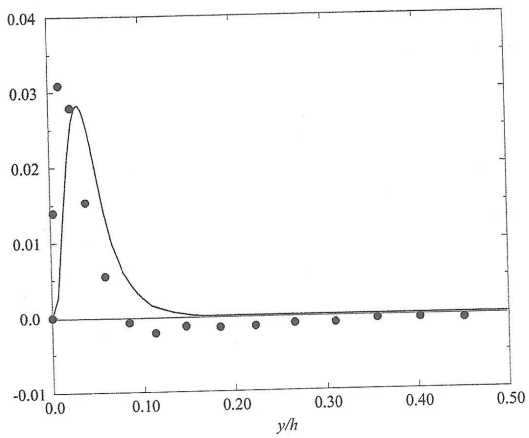

(c)

Fig. 6.18 *Predicted vorticity fluxes: •, DNS results; —, prediction from Eqs. (6.39) through (6.42). (c)* $\overline{w\omega_1}$. *(From [1]. Copyright © Springer-Verlag.)*

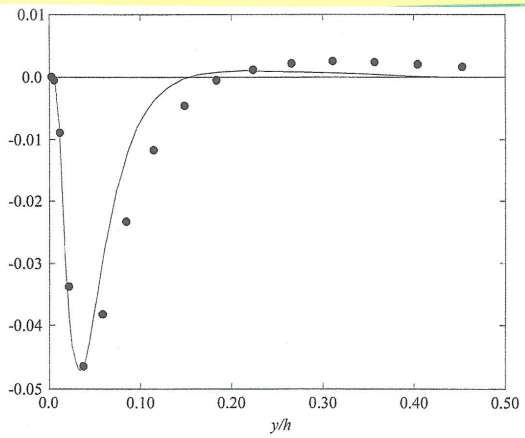

(d)

Fig. 6.18 *Predicted vorticity fluxes: •, DNS results; —, prediction from Eqs. (6.39) through (6.42). (d)* $\overline{w\omega_2}$. *(From [1]. Copyright © Springer-Verlag.)*